AGRICULTURE AND NATURAL RESOURCES

Journal homepage: http://anres.kasetsart.org

Research article

Effect of various phosphate fertilizers on growth and antioxidant activity of *Euglena gracilis* Klebs, 1883 IDN22 isolated from Dieng Peatland, Indonesia

Eko Agus Suyono[a,d,*], Arief Budiman[b,c,d,†], Nugroho Dewayanto[c,d,†], Indira Amani Kurniawan[a,†], Laila Mei Marwadani[a,†], Renisha Windy Puspita Sari[a,†], Sri Setyaningrum[a,†], Renata Adaranyssa Egistha Putri[e,†]

[a] *Faculty of Biology, Universitas Gadjah Mada, Yogyakarta 55281, Indonesia*

[b] *Department of Chemical Engineering, Faculty of Engineering, Universitas Gadjah Mada, Yogyakarta 55281, Indonesia*

[c] *Master of System Engineering Program, Faculty of Engineering, Universitas Gadjah Mada, Yogyakarta 55281, Indonesia*

[d] *Center of Excellent of Microalgae Biorefinery, Center for Energy Studies, Universitas Gadjah Mada, Yogyakarta 55281, Indonesia*

[e] *Study Program of Biotechnology, Graduate School of Universitas Gadjah Mada,Yogyakarta 55281, Indonesia*

Article Info

Article history:
Received 25 March 2025
Revised 27 August 2025
Accepted 28 August 2025
Available online 29 September 2025

Keywords:
Antioxidant activity,
Euglena gracilis,
Microalgae,
Phosphate fertilizer,
Pigment

Abstract

Importance of the work: A cost-efficient, phosphate fertilizer-based medium could improve the economic feasibility of *Euglena gracilis* Klebs, 1883 production for food industry applications.
Objectives: To assess the effect of different phosphate fertilizer types on the growth and antioxidant activity of the indigenous isolate *E. gracilis* IDN22.
Materials and Methods: Batch cultivation (150 L) of the local isolate *E. gracilis* IDN22 was conducted in separate tanks for each treatment, using media supplemented with various phosphate fertilizers: triple super phosphate (TSP), diammonium phosphate (DAP), monoammonium phosphate (MAP) and fused magnesium phosphate (FMP). Technical replicates (n = 3) were collected for the analysis. The observed variables were: cell growth (measured using a Neubauer counting chamber); biomass production (using the filtration method); pigment concentration and productivity (analyzed using spectrophotometry); and antioxidant activity (assessed using the 2,2 diphenyl-1-picrylhydrazyl method based on half maximal inhibitory concentration (IC_{50}) values).
Results: The DAP treatment produced the highest cell density in the exponential phase on day 13, while the MKP treatment had the highest growth rate (μ_{max} = 0.736). In contrast, the FMP treatment had the highest values for biomass content, pigment productivity and absolute pigment. In addition, the MKP treatment had the highest antioxidant activity (IC_{50} = 4.172 mg/mL), while FMP had the lowest antioxidant activity (IC_{50} = 12.647 mg/mL).
Main finding: The findings offer a scientific basis for selecting fertilizers that support sustainable and efficient microalgae production for food industry applications.

† Equal contribution.

* Corresponding author.
E-mail address: eko_suyono@ugm.ac.id (E. Suyono)

https://doi.org/10.34044/j.anres.2025.59.5.11

Introduction

Euglena gracilis Klebs, 1883 is a eukaryotic microalgae that thrives in various aquatic environments, including both marine and freshwater habitats (Kottuparambil et al., 2019). Notably, *E. gracilis* demonstrates remarkable adaptability to extreme conditions, such as high or low temperatures, acidic pH, nutrient deficiency and osmotic stress (Abiusi et al., 2022). This resilience has led to extensive research and applications of *E. gracilis* in the food, cosmetic and pharmaceutical industries (Kottuparambil et al., 2019).

Microalgae contain a wide range of metabolites, including lipids, amino acids, vitamins, minerals, pigments, carbohydrates and paramylon as a carbohydrate reserve (He et al*.,* 2021). *E. gracilis* also produces bioactive compounds and according to Wang et al. (2023), *E. gracilis* is a potential source of natural antioxidants, such as carotenoids and phenols. Other studies have shown that 1,3-β-glucan in *E. gracilis* functions as an immunostimulant that can provide natural protection against parasites (Perveen et al., 2021). Additionally, *E. gracilis* produces β-carotene, α-tocopherol and phytotoxin compounds, which serve as raw materials for pharmaceuticals, cosmetics and nutraceuticals (Kottuparambil et al., 2019). According to Santek et al. (2012), *E. gracilis* can achieve high biomass concentration at low levels of pH and metabolite production. For example, biomass concentrations of approximately 13–14 g/L were obtained at a low pH of 3 in synthetic media, indicating robust growth under acidic conditions. In addition, studies have shown that *E. gracilis* can tolerate and even thrive under stressful conditions, such as a low pH, which can help in mitigating issues related to environmental stressors (Vadlamani et al., 2017; Bernard and Gueguen, 2022)

E. gracilis can survive using only pond water, light and carbon dioxide from its surroundings (Lei et al., 2024). However, optimal growth requires a nutrient-rich culture medium composed of macronutrients, micronutrients and vitamins, with nitrogen (N) and phosphorus (P) being the primary macronutrients essential for microalgae metabolism (Budiman et al., 2023). In natural waters, phosphate is often a limiting nutrient because it readily binds to ions such as CO_3^{2-} and Fe^{3+}, forming precipitates that are difficult for microalgae to absorb Kerr et al., 2011: Oliveira et al., 2011). Generally, microalgae absorb inorganic phosphate forms, such as $H_2PO_4^-$ and HPO_4^{2-}, and can store phosphate as polyphosphate, enabling them to overcome phosphate limitation, detoxify metals and purify wastewater (Wei, 2024).

Optimizing the production of *E. gracilis* biomass and metabolites can be achieved through various cultivation strategies, where factors, such as culture conditions, nutrient supply and variations in light intensity, temperature, pH and salinity, influence the quantity and type of metabolites produced by *E. gracilis* (Abiusi et al., 2022). In recent years, there has been a rapid frown in research on the utilization of microalgae based on nutrient optimization According to Bossa et al., (2024), microalgae have potential applications in wastewater treatment and nutrient recovery due to their ability to accumulate phosphorus, with microalgae having the ability to adapt to phosphorus limitation through increased use efficiency and metabolic modification. In addition, recent studies have highlighted the potential of cost-effective phosphorus sources, such as agro-industrial byproducts (including phytic acid from rice bran) and lignocellulosic sugar alcohols (including mannitol and xylitol), to enhance *E. gracilis* biomass and lipid yields (Zhu et al., 2019; Zhu and Wakisaka, 2020). For example, phytic acid not only serves as a P source but also upregulates phytase activity in *E. gracilis*, improving phosphate assimilation and stress tolerance (Zhu and Wakisaka, 2019).

Often, research on *E. gracilis* uses isolates from foreign sources, which may not be well adapted to cultivation in Indonesia. Successful cultivation and utilization in Indonesia require a deeper understanding of the factors that affect its growth and metabolite production. The *E. gracilis* strain isolated from the Dieng Peatland represents a unique ecological variant due to its adaptation to extreme environmental conditions, namely, acidic pH, nutrient-poor and low-oxygen conditions, which are characteristic of highland tropical peatlands (Maysarah et al., 2021). Unlike other *E. gracilis* strains typically found in freshwater environments, this strain thrives in conditions with high humic substance content, low light penetration and acidic media. This tolerance to acidity is noted as potentially reducing the risk of contamination during cultivation, which is a practical advantage. Beyond its ecological resilience, this Indonesian strain, specifically isolated from Dieng Peatland water, demonstrates valuable biochemical traits. For example, it is capable of producing substantial amounts of metabolites, notably paramylon and wax ester, when cultivated mixotrophically with 10 g/L molasses (Erfianti et al., 2023) . In addition, the strain's natural lack of cell walls, a characteristic feature of *Euglena*, is noted as facilitating the extraction of these valuable metabolites (Astiti et al., 2025).

While other studies have explored the effects of organic P sources, there is a lack of published information on the comparative efficacy of affordable conventional phosphate fertilizers. Therefore, the current study aimed to evaluate the effects of TSP (triple super phosphate fertilizer), DAP (diammonium phosphate fertilizer), MAP (monoammonium phosphate fertilizer) and FMP (fused magnesium phosphate fertilizer) as inorganic P sources on the growth kinetics, pigment production and antioxidant activity of indigenous isolate *E. gracilis* IDN22 in outdoor batch cultures. The findings should contribute to the development of sustainable and cost-effective bioprocesses for producing high-value *E. gracilis*-based products as a source of functional food.

Materials and Methods

Ethics statement

This study did not involve human or animal subjects. The cultivation and experimentation of the local isolate *E. gracilis* were conducted in accordance with institutional biosafety regulations and standard laboratory practices. All procedures followed relevant guidelines for the safe handling of microalgae cultures.

Materials

The microalgae used in this study were sampled from the indigenous strain *E. gracilis* IDN22, isolated from the Dieng Peatland, Indonesia. F1 medium was used for nutrient cultivation, with its composition detailed in Table 1 (Suyono et al., 2023). Additional materials included distilled water, Whatman GF/C filter paper and the following phosphate fertilizers: TSP (Meroke®; 46% P_2O_5, 15% CaO), FMP (Phosgro®; 20% P_2O_5, 20% CaO, 3% MgO), MKP (Pak Tani®; 52% P_2O_5, 34% K2O) and DAP (Pak Tani®; 60% P_2O_5, 12% N).

Table 1 Formulation of F1 medium

Component	Concentration (L)
ZA fertilizer ($(NH_4)_2SO_4$)	1 g
KCl	0.002 g
TSP fertilizer ($Ca(H_2PO_4)_2$)	0.99 g
$MgSO_4$	0.2 g
Trace metal	100 μL
Na_2MoO_4	100 μL
Vitamin B_1	0.1 μL
Vitamin B_{12}	0.0005 μL

Cultivation of E. gracilis

The *E. gracilis* isolated from the Dieng Peatland is maintained as a stock culture at the Laboratory of Biotechnology, Faculty of Biology, Universitas Gadjah Mada, Indonesia, under the code IDN22. In the current study, the *E. gracilis* isolate Dieng IDN22 was cultured through batch culture in stages, starting with mixing 37.5 L of culture inoculum into 112.5 L of F1 medium (1:4 ratio), so that the initial culture volume was 150 L. Each treatment was conducted with technical replicates (n = 3) to minimize technical variation. The physical and chemical conditions during cultivation were controlled in a medium pH of 3.5, according to the F1 medium specifications in Table 1. The average temperature during the cultivation period was in the range 31–33°C. The light intensity was monitored using a lux meter during daylight hours, with recorded values in the range 1,038–1,136 W/m^2. The cultivation process lasted 15 d until the population decline phase was reached.

Data collection

Measurement of cell density

The growth of *E. gracilis* was assessed using the manual cell counting method with a 1 nm Neubauer hemocytometer. Each sample (1 mL) was fixed with alcohol and allowed to stand for 1–2 min. Then, the sample was pipetted into a microscope slide and observed under a light microscope (YS100 Nikon) at 10× magnification (Borowitzka and Moheimani, 2013).

Growth kinetic modeling

Kinetic modeling was used to predict and optimize microalgal growth and to understand better the growth dynamics. The Logistic and Gompertz models, are simple and substrate-independent; they are commonly used to model microbial exponential growth (Galvão et al., 2013). The Logistic model estimates population growth based on the maximum daily growth rate (μ_{max}), while the Gompertz model describes exponential-phase growth using complex parameters such as maximal cell production (r_m) and lag time (t_L). The Logistic model was described using Equations 1 and 2 and the Gompertz model was described using Equation 3 (Galvão et al., 2013):

$$dX|dt = \mu_{max} \times (1 - X / \mu_{max}) \times X \quad (1)$$

$$X = X_0 \exp(\mu_{max} t) / 1 - [x/x_{max} (1-\exp(\mu_{max} t))] \quad (2)$$

$$X = X_0 + [X_{max.}\exp[- \exp ((r_m.\exp(1)/x_{max}) (t_L - t) + 1)]] \quad (3)$$

where X_{max} is the maximum biomass concentration, r_m is the maximal cell production, t_L is the lag time and exp is the exponential function.

In addition to these models, the Richards model offers greater flexibility in representing microalgae growth (Erfianti et al., 2024) The Richards model was selected over simpler options, such as the Logistic and Gompertz models, because, according to Erfianti et al. (2024), it offers enhanced flexibility in modeling asymmetric and sigmoidal growth curves, which more accurately reflect the complex growth behavior of *E. gracilis*. By adjusting the curve shape parameter (v), the Richards model accommodates various growth patterns, including exponential, decelerating and stationary phases (Hsieh, 2009). The Richards model was described using Equation 4 (Hsieh, 2009):

$$dX/dt = \mu_{max} \times X\,(1 - (X / X_{max})^n)\, dX/dt = \mu_{max} \times X\,(1 - (X / X_{max})^n) \quad (4)$$

The coefficient of determination (R^2) was used for appraisal of the models – see Equation (5).

$$R^2 = (1 - SSR / SST) \quad (5)$$

where SSR SSR represents the sum of squared residuals, while SST denotes the sum of squared total (Hsieh, 2009).

Dry weight measurement

The biomass of *E. gracilis* was measured every 3 d during the cultivation period. The biomass was quantified using a filtration method with GF/C filter paper (Whatman, 47 mm). A sample (40 mL) of culture was filtered and dried in an oven at 90°C for 20 min. Then, the dried biomass was weighed using an analytical balance (AE 240; Mettler Toledo). The biomass concentration was calculated using Equation 6:

$$\text{Biomass (mg/mL)} = (\text{Total weight} - \text{Initial Weight}) \times (\text{Sample Volume})^{-1} \quad (6)$$

Pigment content analysis

The pigment was measured every 3 d during the cultivation period using spectrophotometry. A 50 mL sample was centrifuged at 3,300 revolutions per minute (rpm) for 15 min. The supernatant was discarded and acetone was added to the pellet. After homogenization, 2 mL of the solution was analyzed at absorbance wavelengths of 470 nm, 645 nm and 662 nm (Indahsari et al., 2022). Measurements (in milligrams per milliliter) were recorded for both the chlorophyll content using Equations 7–8 and for the carotenoid contents using Equations 9. The total chlorophyll (measured in grams per liter) was calculated using Eqs. 7–9 and Equation 10 respectively:

$$\text{Chl } a = [11.75 \times (A\,662) - 2.350 \times (A\,645) \times 10^{-3})] \quad (7)$$

$$\text{Chl } b = [18.61 \times (A\,645) - 3.960 \times (A\,662) \times 10^{-3})] \quad (8)$$

$$\text{Total Chl} = \text{Chl } a + \text{Chl } b \quad (9)$$

$$\text{Car} = [1{,}000 \times (A\,470) - 2.270 \times \text{Chl } a - 81.4 \times \text{Chl } b / 227] \quad (10)$$

where A_{662} and A_{645} are the absorbance values at the specified wavelength.

The pigment productivity (measured in milligrams per milliliter per day) was calculated using Equation 11:

$$\text{Pigment productivity} = (X_t - X_0) \times (\Delta_t)^{-1} \quad (11)$$

where, $x_{t\,i}$ is the concentration of the pigment at time *t*, x_0 is the concentration of the pigment at the initial time (t = 0) and Δt is the time interval between *t* and *t* = 0 and concentrations were measured in milligrams per milliliter.

Antioxidant activity

The antioxidant activity was measured using the 2,2 diphenyl-1-picrylhydrazyl (DPPH) method on microalgae wet pellet samples. Extraction of wet pellets was carried out using ethanol. Each sample was centrifuged at 4,000 rpm and the supernatant was mixed with 1 mL of 0.4 mM DPPH solution and 4 mL of ethanol. The mixture was incubated at room temperature for 30 min. Then, the absorbance was measured at 515 nm using spectrophotometry (Genesys 150 UV-Vis; Thermo Fisher Scientific). The inhibition percentage was calculated using Equation 12:

$$\%\text{Inhibition} = (\text{Control absorbance-Sample absorbance}) \times (\text{Control absorbance})\text{-}1 \quad (12)$$

The half maximal inhibitory concentration (IC_{50}) value was determined based on the % inhibition using linear regression analysis based on Equation 13:

$$Y = a + bX \quad (13)$$

where Y is the dependent variable (% inhibition), X is the independent variable (sample concentration), a is the y-axis intercept and b is the regression slope coefficient.

Statistical analysis

Data were analyzed using the Excel (version 2021, Microsoft Corp.) and IBM SPSS Statistics (version 27; IBM Corp.) software packages. Statistical testing was performed using one-way analysis of variance (ANOVA) at the 95% confidence level, with significant differences tested at $p < 0.05$ and highly significant differences tested at $p < 0.001$. Mean differences were assessed using Duncan's multiple range test in the IBM SPSS Statistics software. Graphical data visualization was conducted using the OriginPro 2024b (version 2024b; OriginLab) software for clearer presentation of results.

Results

Cell growth rate

Cell density

The growth of *E. gracilis* IDN22 was assessed based on the cell density and biomass content, with the results visualized in Figs. 1–2. Fig. 1 illustrates the growth pattern of *E. gracilis* IDN22 under different fertilizer treatments. All treatments produced a rapid adaptive response, with an almost undetectable lag phase, followed by the early onset of the exponential phase on day 1 of cultivation. Mean peak cell densities on day 10 were recorded for TSP ($16.7 \times 10^4 \pm 0.43$ cells/mL), FMP ($18.5 \times 10^4 \pm 0.99$ cells/mL) and MKP ($18.5 \times 10^4 \pm 0.76$ cells/mL). Notably, the DAP treatment attained a final cell density of $19.3 \times 10^4 \pm 0.38$ cells/mL on day 13, appearing greater than that of the other treatments.

Biomass content

The dry weight measurements of *E. gracilis* IDN22 across the different phosphate fertilizer treatments were analyzed using one-way ANOVA, which revealed highly significant differences ($F_{(3, 8)} = 273.90$, $p < 0.001$, effect size (η^2) = 0.99 for day 12; $F_{(3, 8)} = 180.06$, $p < 0.001$, $\eta^2 = 0.99$ for day 15). Fig. 2 shows that all three treatments produced higher daily biomass contents than the control. The highest biomass contents were on day 15 for the TSP (0.068 ± 0.001 mg/mL), MKP (0.065 ± 0.001 mg/mL) and DAP (0.083 ± 0.001 mg/mL) treatments. In contrast, the FMP treatment reached its peak on day 12 (0.088 ± 0.001 mg/mL), which was higher than the control and the other treatments throughout the cultivation period.

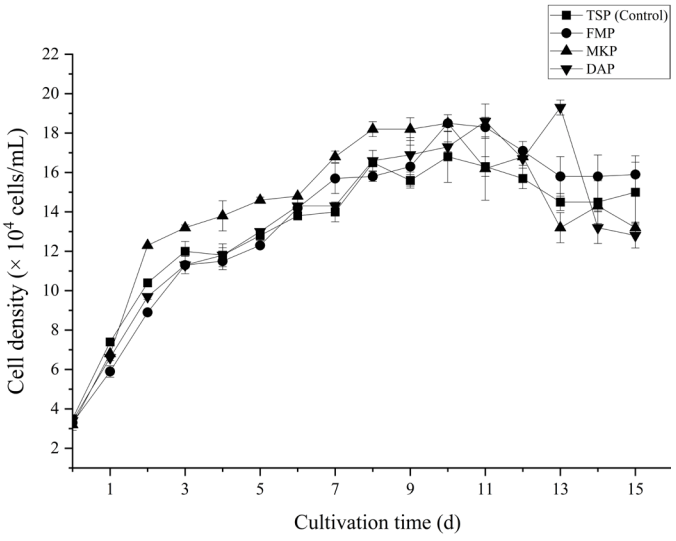

Fig. 1 Growth curve of *Euglena gracilis* under phosphate treatments from different fertilizers during 15 d of cultivation. TSP = triple super phosphate; FMP = fused magnesium phosphate; MKP = mono kalium phosphate); DAP (diammonium phosphate). Error bar = ±SD.

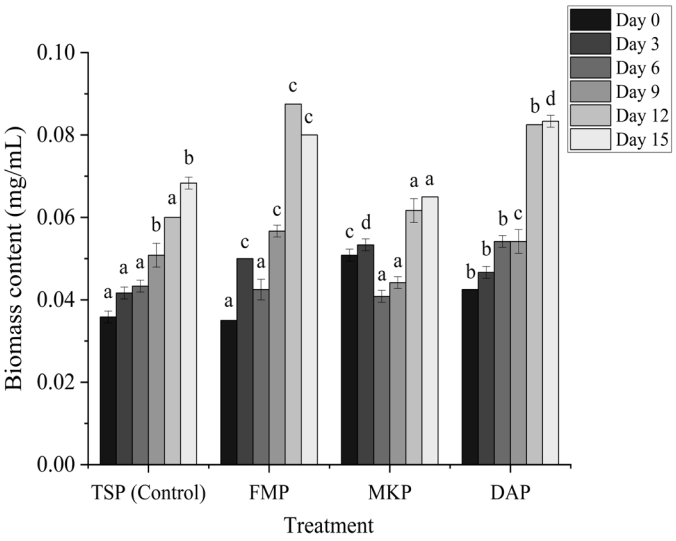

Fig. 2 Dry weight of *Euglena gracilis* IDN22 under various phosphate fertilizer treatments. Bars and error bars represent mean and ±SD, respectively. Different lowercase letters above bars indicate significant differences ($p < 0.05$) among sampling days within each treatment. TSP = triple super phosphate; FMP = fused magnesium phosphate; MKP = mono kalium phosphate; DAP diammonium phosphate.

Growth kinetic modeling

Growth kinetic modeling was applied to better understand and optimize microalgal growth. The results from using the Logistic, Gompertz and Richards models to predict growth trends are shown in Fig. 3. Among the models tested, the Richards model produced the best fit for all treatments, based on the R^2 values, with values for the TSP, FMP, MKP and DAP treatments of 0.935, 0.951, 0.837 and 0.841, respectively. According to the Richards model, the MKP treatment produced the fastest growth rate (μ_{max} = 0.002/d). The FMP treatment produced the highest cell density, with an asymptotic maximum (A) of 17.022 cells/mL. The shape parameters (V) for the TSP, FMP and MKP treatments were positive, while the DAP treatment had a negative value. The t_L values for TSP, FMP, MKP and DAP were all negative (−1.560/d, −1.448/d, −0.687/d and −1.466/d, respectively).

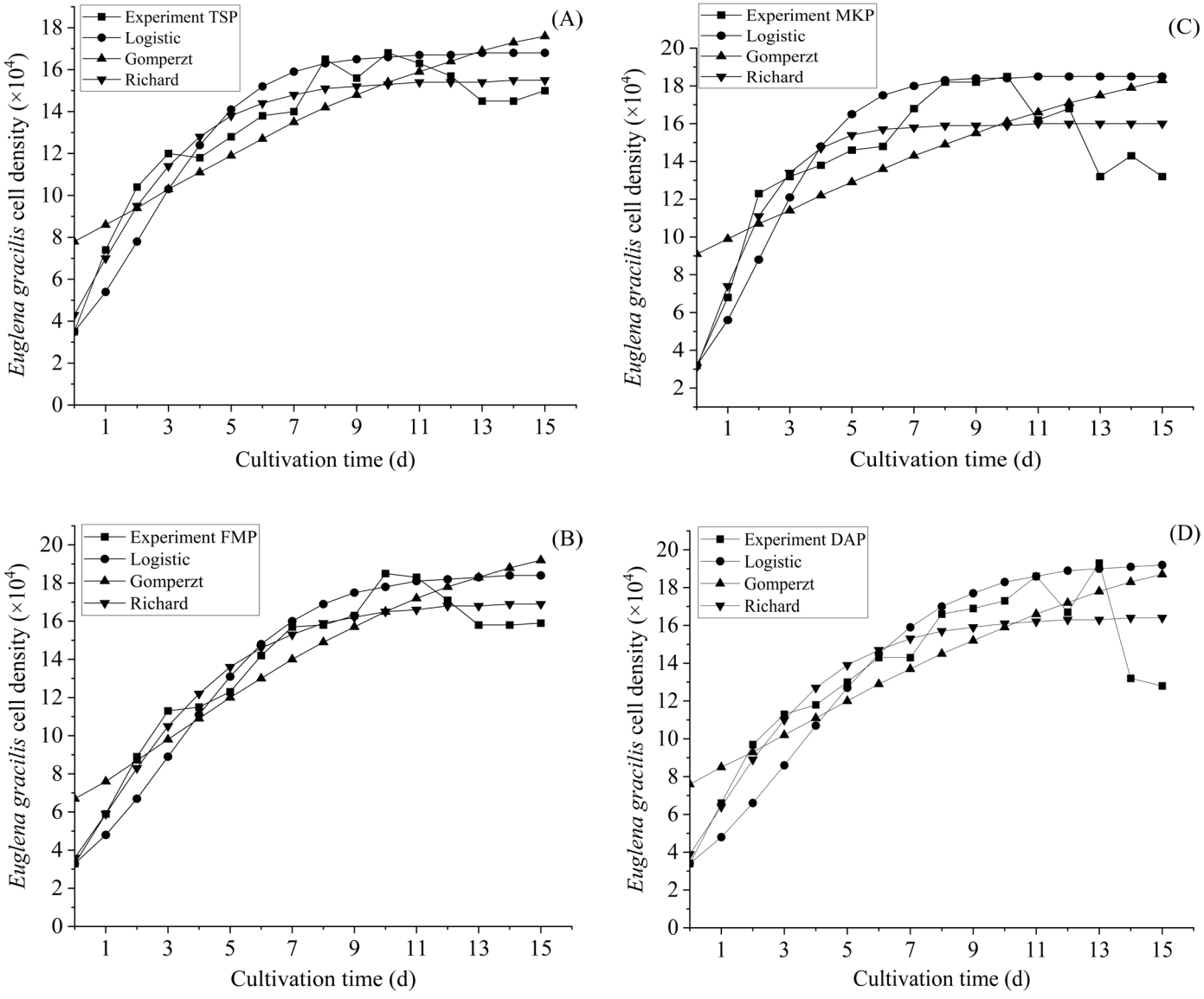

Fig. 3 Growth curves for Logistic, Gompertz, and Richards models for *E. gracilis* cell density, for different fertilizer treatments: (A) triple super phosphate; (B) fused magnesium phosphate; (C) mono kalium phosphate); (D) diammonium phosphate. Error bar = ±SD.

Metabolite content of E. gracilis

Absolute pigment

Data on chlorophyll *a*, chlorophyll *b* and carotenoids were used to calculate both absolute concentration values and pigment productivity. Pigment productivity was assessed to determine the production rate of chlorophyll and carotenoid pigments for each treatment. The results are presented in Tables 2-4.

The absolute concentration of chlorophyll *a* varied among treatments (Table 2). FMP had the highest value (0.506 ± 0.118 µg/mL), but it was not significantly different from either TSP (0.445 ± 0.015 µg/mL) or DAP (0.435 ± 0.031 µg/mL).

Table 2 Absolute concentration value and productivity of chlorophyll *a* pigment under different phosphate fertilizer treatments.

Treatment	Chlorophyll *a* absolute (µg/mL)	Chlorophyll *a* productivity (µg/mL/d)
TSP	0.445±0.015^{ab}	0.030±0.001^{ab}
FMP	0.506±0.118^{b}	0.042±0.010^{b}
MKP	0.328±0.018^{a}	0.027±0.002^{a}
DAP	0.435±0.031^{ab}	0.029±0.002^{a}

Mean ± SD (n = 3) within each column with different lowercase superscripts are significantly different ($p < 0.05$) based on Duncan's multiple range test. Error bar = ±SD.
TSP = triple super phosphate; FMP = fused magnesium phosphate; MKP = mono kalium phosphate); DAP (diammonium phosphate).

Table 3 Absolute concentration value and productivity of chlorophyll *b* pigment under different phosphate fertilizer treatments.

Treatment	Chlorophyll *b* absolute (µg/mL)	Chlorophyll *b* productivity (µg/mL/d)
TSP	0.308±0.015^{b}	0.021±0.001^{a}
FMP	0.528±0.053^{c}	0.044±0.004^{c}
MKP	0.235±0.010^{a}	0.020±0.001^{a}
DAP	0.305±0.011^{b}	0.025±0.001^{b}

Mean ± SD (n = 3) within each column with different lowercase superscripts are significantly different ($p < 0.05$) based on Duncan's multiple range test. Error bar = ±SD.
TSP = triple super phosphate; FMP = fused magnesium phosphate; MKP = mono kalium phosphate); DAP (diammonium phosphate).

Table 4 Absolute concentration values and productivity of carotenoid pigment under different phosphate fertilizer treatments.

Treatment	Carotenoid absolute (mg/mL)	Carotenoid productivity (mg/mL/d)
TSP	0.0618±0.0018^{b}	0.004±0.001^{b}
FMP	0.0654±0.0090^{b}	0.005±0.004^{c}
MKP	0.0471±0.0018^{a}	0.00±0.001^{a}
DAP	0.0515±0.0037^{a}	0.004±0.001^{b}

Mean ± SD (n = 3) within each column with different lowercase superscripts are significantly different ($p < 0.05$) based on Duncan's multiple range test. Error bar = ± SD.
TSP = triple super phosphate; FMP = fused magnesium phosphate; MKP = mono kalium phosphate); DAP (diammonium phosphate).

In contrast, the MKP treatment had the lowest concentration value (0.328 ± 0.018 µg/mL) which was significantly lower than for FMP. A slightly different pattern was observed for chlorophyll *a* productivity (Table 2). FMP (0.042 ± 0.010 µg/mL/d) was higher than MKP (0.027 ± 0.002 µg/mL/d), DAP (0.029 ± 0.002 µg/mL/d) and TSP (0.030 ± 0.001 µg/mL/d), but not significantly different from TSP. Notably, MKP had the consistently lowest values across both parameters.

The absolute concentration of chlorophyll *b* (Table 3) was the highest for FMP (0.528 ± 0.053 µg/mL) and was significantly higher than all the other treatments. TSP (0.308 ± 0.015 µg/mL) and DAP (0.305 ± 0.011 µg/mL) had comparable concentrations, with both significantly higher than MKP (0.235 ± 0.010 µg/mL). Similarly, for productivity (Table 4), FMP had the highest value (0.044 ± 0.004 µg/mL/d) and was significantly higher than all the other treatments. However, DAP (0.025 ± 0.001 µg/mL/dy) had significantly higher productivity than both TSP (0.021 ± 0.001 µg/mL/d) and MKP (0.020 ± 0.001 µg/mL/d), which did not differ significantly from each other.

The carotenoids absolute concentration (Table 4) was the highest for FMP (0.0654 ± 0.0090 mg/mL); however, this was not significantly different from TSP (0.0618 ± 0.0018 mg/mL). Both FMP and TSP were significantly higher than DAP (0.0515 ± 0.0037 mg/mL) and MKP (0.0654 ± 0.0018 mg/mL). For productivity (Table 4), FMP (0.005 ± 0.004 mg/mL/d) was significantly higher than all the other treatments. Consistent with the other pigments, MKP also had the lowest value for both the absolute concentration and productivity of carotenoids.

These findings indicated that while the FMP treatment frequently resulted in elevated pigment levels, these enhancements were not always significant compared to the TSP and DAP treatments. Conversely, the MKP treatment consistently produced the lowest values across all measured pigment parameters, with significant differences from FMP.

Antioxidant activity

The antioxidant activity of *E. gracilis* was evaluated based on IC_{50} values, as shown in Table 5. The MKP-treated sample had the highest antioxidant activity with an IC_{50} value of 4.172 mg/mL. In contrast, the FMP sample had the lowest activity with an IC_{50} value of 12.647 mg/mL. The TSP and DAP samples had moderate antioxidant activity levels, with IC_{50} values of 6.545 mg/mL and 7.825 mg/mL, respectively. Based on these results, the MKP treatment provided the strongest antioxidant properties, while the FMP treatment resulted in the weakest activity.

Table 5 Half maximal inhibitory concentration (IC_{50}) value of *Euglena gracilis* extract.

Phosphate source	IC_{50} (mg/mL)
TSP (control)	6.545 ± 0.098
FMP	12.647 ± 0.177
MKP	4.172 ± 0.064
DAP	7.825 ± 0.115

Data are mean±SD (n = 3). Extract with lowest IC_{50} value =strongest antioxidant activity.
TSP = triple super phosphate; FMP = fused magnesium phosphate; MKP = mono kalium phosphate); DAP = diammonium phosphate.

Discussion

Cell growth rate of E. gracilis

Cell density

Cell density refers to the number of cells per unit volume in a culture and serves as a key indicator for assessing growth performance and treatment effectiveness. In this study, daily cell density measurements were recorded using a Neubauer counting chamber, following the hemocytometry method to construct a growth curve (Fig. 1). Typically, the growth curve includes distinct phases that reflect changes in the culture's physicochemical conditions over time (Zhou et al., 2017). Growth begins with the lag phase, during which cells adapt to new conditions by synthesizing essential enzymes before initiating cell division. Consequently, little to no increase in cell density occurs during this phase (Zhou et al., 2017). As shown in Figure 1, the lag phase in the current study was barely noticeable across all treatments, suggesting that *E. gracilis* adapted quickly to the cultivation conditions.

Following adaptation, the culture enters the exponential phase, marked by rapid cell division and a sharp increase in cell density due to sufficient nutrient availability (Cordova et al., 2018). In the current study, the exponential phase began on day 1 of cultivation, with the TSP, FMP and MKP treatments, reaching peak cell density on day 10. In contrast, the DAP treatment peaked on day 13, achieving the highest cell density among all treatments. The increased cell density under the DAP treatment may be attributed to its high phosphate content (60%), as shown in Table 6. Phosphate plays a vital role in synthesizing key biomolecules such as ATP, DNA, RNA and phospholipids (Bossa et al., 2024). Furthermore, adequate phosphate availability supports essential metabolic processes, facilitating continuous cell growth. The high phosphate content in DAP likely prevented nutrient limitations throughout the cultivation period, enabling sustained cellular development.

The exponential phase is marked by the highest metabolic activity. However, as nutrients are depleted and metabolic byproducts accumulate, the culture enters the linear phase, where the growth rate begins to decline. Continued nutrient limitation and the buildup of toxic byproducts lead to the decline phase, during which cell proliferation slows noticeably. This is followed by the stationary phase, where a balance is maintained between cell division and cell death. Eventually, the culture reaches the death phase, characterized by nutrient exhaustion and increasingly toxic conditions, causing cell death to exceed proliferation and leading to a sharp decline in the population (Cordova et al., 2018).

Biomass content

The biomass content refers to the total biological material produced by microalgae during cultivation, including living cells and cellular components such as proteins, lipids and carbohydrates. In the current study, the highest biomass was in the FMP treatment on day 12 (Fig. 2), which was significantly different from the other treatments, indicating that FMP was effective in supporting the growth and biomass accumulation of the *E. gracilis* IDN22 strain from Dieng.

FMP is a slow-release phosphate fertilizer that provides a steady and continuous supply of phosphate (Lubkowski, 2016). This consistent nutrient availability throughout the cultivation period supports sustained cell growth and can greatly enhance biomass production. In addition, the controlled release of phosphate helps prevent early nutrient overload, which can otherwise inhibit growth or lead to the accumulation of toxic metabolic byproducts. In the current study, the impact of FMP on the biomass content was reflected in its earlier peak on day 12, while the other treatments reached their peak on day 15. This suggested that the gradual phosphate release from FMP enabled the culture to maintain a high growth rate and reach the stationary phase sooner. Therefore, FMP not only improved the biomass yield but also shortened the cultivation duration. Supporting this, other studies have provided insight into the dynamics of phosphate supply and its impact on biomass.

Table 6 Phosphate source by cultivation treatment

Phosphate source (L)	Concentration (g/L)
TSP, (0.2 g P; 0.1 g Ca)	1
FMP, (0.08 g P; 0.14 g Ca; 0.02 g Mg)	1
MKP, (0.23 g P; 0.28 g K)	1
DAP, (0.26 g P; 0.12 g N)	1

TSP = triple super phosphate; FMP = fused magnesium phosphate; MKP = mono kalium phosphate); DAP = diammonium phosphate.

For example, Beuckels et al. (2013) reported that adding FMP (which initially released low amounts of phosphorous but gradually increased its availability over time) induced flocculation, which is essential for efficient biomass recovery. The slow release of essential nutrients from FMP ensures a sustained nutrient supply, supporting continuous nutrient uptake and metabolic activity in microalgae. This steady provision of minerals may promote more consistent growth and thus enhance overall biomass production (Hou et al., 2019; Suleiman et al., 2020; Fichtbauer et al., 2025).

In contrast, MKP is a high-release phosphate fertilizer that dissolves rapidly at the beginning of cultivation (Jalali et al., 2022). While this may promote rapid initial growth, the quick depletion of phosphate can lead to nutrient limitations in later stages. As a result, cell growth slows and biomass accumulation does not reach its full potential.

Growth kinetic modeling

The R^2 coefficient is a statistic that indicates how well a model fits the experimental data (Phukoetphim et al., 2017). Based on the kinetic modeling results (Fig. 3), all treatments demonstrated that the Richards model provided the best fit to the experimental data, as shown by the R^2 values in Table 7. The Richards model is a flexible mathematical approach for describing population growth, particularly in microorganisms. This model adjusts the curve shape parameter (V) to capture different growth phases—exponential, decelerating and stationary—where the maximum specific growth rate (μ_{max}) and the maximum cell density (X_{max}) are key parameters. Compared to the Logistic or Gompertz models, the Richards model offers a better fit for optimizing microalgal cultivation (Setiantoro et al., 2024). The Logistic model describes growth that begins exponentially but slows as it approaches the system's carrying capacity. In contrast, the Gompertz model describes growth that starts rapidly but decelerates exponentially over time (Phukoetphim et al., 2017).

The variable μ_{max} represents the highest rate of population increase under optimal conditions, reflecting how quickly microalgae can grow in favorable environments (Erfianti et al., 2024). While both the Logistic and Richards models include a parameter denoted as $\mu_{max,}$ their biological interpretations differ fundamentally. In the Logistic model, μ_{max} represents the absolute maximum growth rate during the exponential phase. However, in the Richards model, μ_{max} serves as a scaling parameter within a flexible sigmoidal function, where the actual growth dynamics are governed by its interaction with additional shape parameters (A, ν). Here, μ_{max} does not directly reflect the empirical growth rate but instead modulates the inflection point and asymmetry of the curve. For example, even a numerically small μ_{max} value (such as 0.002/d for MKP) can yield a biologically plausible growth trajectory when combined with appropriate A and ν values, as evidenced by the model's superior fit (higher R^2 values in Table 7).

Based on the Richards model (Table 7), the positive μ_{max} values in the TSP, FMP and MKP treatments indicated successful population growth, with MKP achieving the fastest growth rate, followed by FMP and TSP. In contrast, a negative μ_{max} in the DAP treatment indicated population decline, suggesting that DAP was not effective in supporting *E. gracilis* growth under these conditions. The MKP treatment produced the highest growth among all treatments (μ_{max} = 0.736), indicating its ability to supply readily available nutrients to support cell division. MKP contained the second-highest phosphate content (52%) after DAP and also provided 34% potassium (K_2O), as shown in Table 6. Potassium functions as an essential cofactor in enzymatic reactions and plays a role in activating more than 60 enzymes associated with growth, with the intracellular concentration of potassium influencing the number of enzymes that can be activated (Iyer et al., 2015).

Table 7 Growth rate parameters of Logistic, Gompertz and Richards models

Model	Parameter	TSP	FMP	MKP	DAP
Logistic	μmax	0.594	0.483	0.736	0.440
	r^2	0.808	0.872	0.562	0.619
Gompertz	rm	0.851	1.104	0.785	0.894
	tl	-4.976	-2.861	-7.492	-4.621
	r^2	0.713	0.810	0.422	0.630
Richards	μmax*	0.001	0.001	0.002	-0.0004
	A	15.476	17.002	15.958	16.417
	v	0.0002	0.0001	0.0001	-0.00007
	tl	-1.560	-1.448	-0.687	-1.466
	r^2	0.935	0.951	0.837	0.841

TSP = triple super phosphate; FMP = fused magnesium phosphate; MKP = mono kalium phosphate); DAP = diammonium phosphate.

* Values derived from Richards model and not directly comparable to Logistic model μ_{max} due to differences in model structure.

The asymptotic maximum (A) represents the upper limit of population growth, where the growth rate slows and the population approaches equilibrium. In the Richards model, this value corresponds to the maximum cell density (X_{max}), or the carrying capacity of the culture environment. Based on Table 3, the FMP treatment had the highest cell density, followed by DAP, MKP and TSP. This asymptotic maximum reflects the environmental carrying capacity and the potential limit of microalgal population growth under different treatment conditions (Tian et al., 2020).

The shape parameter (V) determines the form of the growth curve and influences its symmetry to accommodate various growth patterns (Tian et al., 2020). Based on the Richards model (Table 7), the positive shape parameter values in the TSP, FMP and MKP treatments indicate accelerated growth trends. In contrast, the negative value in the DAP treatment suggests an initial rapid growth phase followed by a decline toward the end of the cultivation period. Biologically, this parameter reflects how rapidly a population transitions from exponential to stationary growth. A positive V implies a sustained exponential phase and more efficient nutrient utilization, whereas a negative V may indicate early nutrient depletion or stress-induced deceleration (Molski, 2025). In the current study, the positive V values in the TSP, FMP and MKP treatments signified favorable growth dynamics, while the negative V in DAP suggested a possible early stress response or suboptimal phosphate assimilation by *E. gracilis*.

Lag time (tL) refers to the delay before the onset of exponential growth, reflecting the period required for cells to adapt to a new environment before active proliferation begins (Altas, 2009). According to the Richards model (Table 7), the negative lag time values across treatments suggested that *E. gracilis* adapted rapidly to the cultivation environment. Among all treatments, MKP had the shortest lag time (−0.687/d), indicating the fastest adaptation and initiation of growth compared to the others.

Metabolite content of E. gracilis

Pigment analysis

E. gracilis is a highly adaptable microalga that produces primary metabolites essential for cellular defense, photosynthesis and stress responses, while also synthesizing secondary metabolites, such as chlorophyll and carotenoids, in response to environmental stress or biotic stressors (Nurafifah et al., 2023).

Table 2 and Table 3 show that the FMP treatment had higher absolute concentration values and productivity for both chlorophyll *a* and chlorophyll *b*, respectively, although these increases were not always significant compared to the TSP and DAP treatments. Despite its low phosphate content (20%), FMP contains magnesium (Mg), which may have contributed to the increased chlorophyll synthesis. Chemically, chlorophyll does not contain phosphorus (P) in its structure but incorporates magnesium (Mg) and nitrogen (N) as key components (Poblete et al., 2025). In addition to its structural role, chlorophyll plays a critical role in photosynthesis by capturing light energy for ATP production. Under phosphate-limited conditions such as those in the FMP treatment, cells may adapt by enhancing chlorophyll synthesis to maximize light capture, even if ATP production is reduced (Elango et al., 2023). This adaptation likely explains the elevated chlorophyll levels observed in the FMP treatment.

Conversely, the MKP treatment resulted in consistently significant lower concentrations and productivity of both chlorophyll *a* and *b*. MKP contains 52% phosphate, the second highest after DAP (60%). However, MKP lacks components involved in chlorophyll biosynthesis (unlike DAP, which supplies both phosphate and ammonium nitrogen through its diammonium phosphate composition) (Poblete et al., 2025). The absence of these supporting elements may have limited chlorophyll synthesis in the MKP treatment, resulting in lower pigment accumulation and production rates.

As shown in Table 4, the FMP treatment had the highest carotenoid contents, both in terms of absolute concentration and productivity. However, these values were not significantly different compared to the TSP and DAP treatments, although they resulted in the formation of different subsets in the statistical analysis. The distinction between treatments, as indicated by the subset grouping, reflects the separation of groups based on the significance test. However, the numerical differences in carotenoid productivity among treatments were relatively small and did not demonstrate substantial variation. Thus, although the treatments were statistically categorized into different subsets, the observed differences suggesting limited practical distinction despite statistical categorization.

According to Liyanaarachchi et al. (2020), phosphorus limitation during microalgae cultivation can stimulate increased synthesis of pigments, including carotenoids. This response is related to the diversion of cellular energy from growth to pigment production as an adaptive mechanism. The energy flow will switch to the secondary metabolic pathway, namely the isoprenoid pathway, for carotenoid synthesis with its main precursors being isopentenyl pyrophosphate and dimethylalyl pyrophosphate. This response is linked to the redirection

of cellular energy from growth to pigment production as an adaptive mechanism. In particular, carotenoids act as accessory pigments that are commonly upregulated under stress conditions in photosynthesis. Thus, nutrient-limited environments promote higher carotenoid production as a survival strategy.

The pigments of *E. gracilis* serve distinct roles in stress protection. Chlorophyll supports photosynthesis and helps mitigate oxidative stress, while carotenoids function to neutralize free radicals and reduce damage caused by reactive oxygen species (Takaichi, 2025). Therefore, the current study provided new insights into how phosphate limitation affected chlorophyll and carotenoid production.

Antioxidant activity

The IC_{50} value is a measure of a compound's effectiveness in inhibiting a specific biological or biochemical function, representing the concentration required to inhibit 50% of a target activity, where a lower IC_{50} value indicates stronger antioxidant activity (Maitulung et al., 2022). The order of antioxidant strength from highest to lowest was MKP > TSP > DAP > FMP. However, all the IC_{50} values were well above the threshold for even low antioxidant activity. According to Ramadhan et al. (2019), an extract is considered to have very high antioxidant activity if the IC_{50} is < 0.05 mg/mL, high if it in the range 0.05–0.1 mg/mL, moderate if > 0.1–0.15 mg/mL and low if > 0.15–0.2 mg/mL. Based on these criteria, the antioxidant activity of the *E. gracilis* extracts in the current study exceeds the upper limit of the "low" category defined by Ramadhan et al. (2019), indicating that its antioxidant activity falls outside the range of their classification system and can be considered very weak in comparison.

The strength or weakness of antioxidant activity in microalgae is influenced by nutrient availability during cultivation. P is a key macronutrient that plays a vital role in regulating antioxidant enzyme activity, including enzymes such as catalase (CAT), peroxidase and superoxide dismutase. A deficiency in phosphorus can substantially reduce the activity of these enzymes, leading to lower antioxidant capacity (Sun et al., 2021). In the current study, the FMP treatment, which had the lowest P content, also had the lowest antioxidant activity, suggesting that P limitation during cultivation negatively impacted antioxidant activity. Conversely, the DAP treatment, despite having the highest P content, had lower antioxidant activity than both MKP and TSP. This may have been due to excessive P levels, which can lead to toxicity and disrupt cellular metabolism, including the antioxidant defense system (Zhang et al., 2024). Besides P, other factors should be considered. The N content of DAP and the potassium (K) content of MKP can also affect antioxidant activity, especially as K plays an active role in the management of stress response to prevent oxidative damage, as well as playing a role in the regulation of CAT, which is important in the antioxidant defense system (Chrysargyris and Tzortzakis, 2025). This condition may have caused the higher antioxidant activity of MKP compared to DAP.

Conclusion

The FMP treatment consistently had higher levels of biomass content and enhanced production of secondary metabolites, including chlorophyll *a*, chlorophyll *b* and carotenoids. The MKP treatment had the highest growth rate, with a μ_{max} value of 0.736 and the strongest antioxidant activity, with an IC_{50} value of 4.172 ± 0.064 mg/mL. Therefore, The FMP treatment is more suitable in cultivation of *E. gracilis* that aims in high biomass and chlorophyll production, such as materials for food and feed. While the MKP treatment can be chosen if the aim of the cultivation is fast cell growth with high antioxidant activity. Thus, the treatment is recommended to be used in supplement production. Further characterization of *E. gracilis* primary and secondary metabolites is needed to determine the application for those metabolites.

Conflict of Interest

The authors declare no conflicts of interest.

Acknowledgements

The Biotechnology Laboratory and the Karanggayam Biodiversity Research Station II, Faculty of Biology, Universitas Gadjah Mada, Indonesia provided research facilities. Mr. Dedy Kurnianto, Ms. Tia Erfianti, Dr. Ria Amelia and Ms. Ersi Larasati provided valuable assistance.

References

Abiusi, F., Trompetter, E., Pollio, A., Wijffels, R.H., Janssen, M. 2022. Acid tolerant and acidophilic microalgae: an underexplored world of biotechnological opportunities. Front. Microbiol. 13: 820907. doi.org/10.3389/fmicb.2022.820907

Altas, L. 2009. Inhibitory effect of heavy metals on methane-producing anaerobic granular sludge. J. Hazard. Mater. 162: 1551–1556. doi:10.1016/j.jhazmat.2008.06.048

Astiti, A., Erfianti, T., Maghfiroh, K.Q., Putri, R.A.E., Suyono, E.A. 2025. Exploration of lipid profile and wax ester content from local strain *Euglena* sp. IDN33 cultivated in mixotrophic condition combined with molasses supplementation. Hayati J. Biosci. 32: 805–818. doi.org/10.4308/hjb.32.3.805-818

Beuckels, A., Depraetere, O., Vandamme, D., Foubert, I., Smolders, E., Muylaert, K. 2013. Influence of organic matter on flocculation of *Chlorella vulgaris* by calcium phosphate precipitation. Biomass Bioenerg. 54: 107–114. doi.org/10.1016/j.biombioe.2013.03.027

Bernard, E., Guéguen, C. 2022. Influence of carbon sources on the phenolic compound production by *Euglena gracilis* using an untargeted metabolomic approach. Biomolecules 12: 795. doi.org/10.3390/biom12060795

Budiman, A., Suyono, E.A., Merdekawati, A., et al. 2023. Mikroalga: Kultivasi, pemanenan, ekstraksi, dan konversi energi. UGM PRESS. Yogyakarta, Indonesia. [in Indonesian]

Borowitzka, M.A., Moheimani, N.R. 2013. Algae for biofuels and energy. Dordrecht: Springer Netherlands, pp. 273–283.

Bossa, R., Melania, D.C., Giovanna, S., Simona, C. 2024. Phosphorous utilization in microalgae: physiological aspects and applied implications. Plants. 13: 2127. doi.org/10.3390/plants13152127

Chrysargyris, A., Tzortzakis, N. 2025. Optimizing nitrogen, phosphorus, and potassium requirements to improve *Origanum dubium* Boiss. growth, nutrient and water use efficiency, essential oil yield and composition. Ind. Crops Prod. 224: 120291. doi.org/10.1016/j.indcrop.2024.120291

Córdova, O., Ruiz-Filippi, G., Fermoso, F.G., Chamy, R. 2018. Influence of growth kinetics of microalgal cultures on biogas production. Renew. Energy. 122: 455–459. doi.org/10.1016/j.renene.2018.01.125

Elango, T., Jeyaraj, A., Dayalan, H., Arul, S., Govindasamy, R., Prathap, K., Li, X. 2023. Influence of shading intensity on chlorophyll, carotenoid and metabolites biosynthesis to improve the quality of green tea: a review. Energy Nexus. 12: 100241. doi.org/10.1016/j.nexus.2023.100241

Erfianti, T., Yusuf, A.F., Handayani, S., Sadewo, B.R., Daryono, B.S., Budiman, A., Suyono, E.A. 2024. Enhancing growth and metabolite profils in indigenous *Euglena gracilis* through explorative light spectrum effect. Egypt. J. Aquat. Res. 50: 318–331. doi.org/10.1016/j.ejar.2024.09.003

Fichtbauer, A.A., Janssen, M., Barbosa, M. 2025. Membrane assisted algae cultivation for high productivity and nutrient recovery in horticultural drain water. Algal Res. 104056. doi.org/10.1016/j.algal.2025.104056

Galvão, R.M., Santana, T.S., Fontes, C.H.O., Sales, E.A. 2013. Modeling of biomass production of *Haematococcus pluvialis*. Appl. Math. 4: 50–56. doi.org/10.4236/am.2013.48A008

He, J., Liu, C., Du, M., Zhou, X., Hu, Z., Lei, A., Wang, J. 2021. Metabolic responses of a model green microalga *Euglena gracilis* to different environmental stresses. Front. Bioeng. Biotechnol. 9: 662655. doi.org/10.3389/fbioe.2021.662655

Hou, C.H., Miao, J.Y., Gu, S.Y., Wang, H.B., Wang, Y.Y., Xu, X.C. 2019. Innovation of fused calcium magnesium phosphate products to promote industry development. J. Plant Nutr. Fertil. 25: 2162–2169. doi.org/10.11674/zwyf.19172

Hsieh, Y.H. 2009. Richards model: a simple procedure for real-time prediction of outbreak severity. In: Zhien, M., Yicang, Z., Wu, J. Vol. 11. Series in Contemporary Applied Mathematics, pp. 216–236. Higher Education Press. Taiwan.

Indahsari, H.S., Tassakka, A.C.M.A., Dewi, E.N., Yuwono, M., Suyono, E.A. 2022. Effects of salinity and bioflocculation during *Euglena* sp. harvest on the production of lipid, chlorophyll, and carotenoid with *Skeletonema* sp. as a bioflocculant. J. Pure Appl. Microbiol. 16: 25–29.

Jalali, M., Elham, A.F., Mahdi, J. 2022. Simulating phosphorus leaching from two agricultural soils as affected by different rates of phosphorus application based on the geochemical model PHREEQC. Environ. Monit. Assess. 194: 164. doi.org/10.1007/s10661-022-09828-6

Kottuparambil, S., Thankamony, R.L., Agusti, S. 2019. *Euglena* as a potential natural source of value-added metabolites: A review. Algal Res. 37: 154–159. doi.org/10.1016/j.algal.2018.11.024

Latief, M., Tafzi, F., Saputra, A. 2013. Aktivitas antioksidan ekstrak metanol beberapa bagian tanaman kayu manis (*Cinnamomum burmani*) asal kabupaten kerinci provinsi jambi. Prosiding Semirata FMIPA Universitas Lampung. 73–76. [in Indonesian]

Liyanaarachchi, V.C., Nishshanka, G.K.S.H., Premaratne, R.G.M.M., Ariyadasa, T.U., Nimarshana, P.H.V., Malik, A. 2020. Astaxanthin accumulation in the green microalga *Haematococcus pluvialis*: Effect of initial phosphate concentration and stepwise/continuous light stress. Biotechnol. Rep. 18: 538. doi.org/10.1016/j.btre.2020.e00538

Lubkowski, K. 2016. Environmental impact of fertilizer use and slow release of mineral nutrients as a response to this challenge. Pol. J. Chem. Technol. 18: 72–79. doi.org/10.1515/pjct-2016-0012

Maysarah, S., Nugroho, Y., Susilawati. 2021. Analysis of soil physical properties in peatland in Liang Anggang district Banjar Baru city South Kalimantan province. J. Sylva Scienteae. 4: 166–173.

Maitulung, I., Maarisit, W., Pareta, D.N., Lengkey, Y.K. 2022. Uji aktivitas antioksidan ekstrak etanol akar manukan (*Rhinacanthus nasutus* (L) Kurz). Biofarmaset. Trop. 5: 127–134. doi.org/10.55724/jbt.v5i2.383 [in Indonesian]

Molski, M. 2025. Hyperbolic representation of the Richards growth model. Mathematics. 13: 1316. doi.org/10.3390/math13081316

Moussa, D.B., Ines, C., Chtourou, H., Karray, F., Sayadi, S., Dhouib, A. 2017. Nitrogen or phosphorus repletion strategies for enhancing lipid or carotenoid production from *Tetraselmis marina*. Bioresour. Technol. 238: 325–332. doi.org/10.1016/j.biortech.2017.04.008

Nurafifah, I., Hardianto, M.A., Erfianti, T., Amelia, R., Kurnianto, D., Suyono, E.A. 2023. The effect of acidic pH on chlorophyll, carotenoids, and carotenoid derivatives of *Euglena* sp. as antioxidants. Aquac. Aquar. Conserv. Legis. 16: 2391–2401.

Perveen, S., Yang, L., Zhou, S., et al. 2021. β-1,3-Glucan from *Euglena gracilis* as an immunostimulant mediates the antiparasitic effect against *Mesanophrys* sp. on hemocytes in marine swimming crab (*Portunus trituberculatus*). Fish Shellfish Immunol. 114: 28–35. doi.org/10.1016/j.fsi.2021.04.005

Phukoetphim, N., Salakkam, A., Laopaiboon, P., Laopaiboon, L. 2017. Kinetic models for batch ethanol production from sweet sorghum juice under normal and high gravity fermentations: Logistic and modified Gompertz models. J. Biotechnol. 243: 69–75. doi.org/10.1016/j.jbiotec.2016.12.012

Poblete, T., Watt, M.S., Buddenbaum, H., Zarco-Tejada, P.J. 2025. Chlorophyll content estimation in radiata pine using hyperspectral imagery: A comparison between empirical models, scaling-up algorithms, and radiative transfer inversions. Agric. For. Meteorol. 362: 110402. doi.org/10.1016/j.agrformet.2025.110402

Ramadhan, R., Kristianti, A.N., Amirta, R., Kusuma, I.W., Phuwapraisirisan, R., Haqiqi, M.T., Saparwadi, S. 2019. Screening for potential antidiabetes and antioxidant activities of selected plants from East Kalimantan, Indonesia. J. Biol. Divers. 20: 1820–1826. doi.org/10.13057/biodiv/d200705

Šantek, B., Friehs, K., Lotz, M., Flaschel, E. 2012. Production of paramylon, a β-1,3-glucan, by heterotrophic growth of *Euglena gracilis* on potato liquor in fed-batch and repeated-batch mode of cultivation. Eng. Life Sci. 12: 89–94. doi.org/10.1002/elsc.201100025

Schagerl, M., Ludwig, I., El-Sheekh, M., Kornaros, M., Ali, S.S. 2022. The efficiency of microalgae-based remediation as a green process for industrial wastewater treatment. Algal Res. 66: 102775. doi.org/10.1016/j.algal.2022.102775

Setiantoro, A.E., Dewayanto, N., Budiman, A. 2024. Analisis kinetika pertumbuhan mikroalga *Spirulina* sp. menggunakan pemodelan Richard dan Gompertz pada fotobioreaktor Algaetree. J. Ilm. Univ. Batanghari Jambi. 24: 1424–1428. doi.org/10.33087/jiubj.v24i2.5369 [in Indonesian]

Suleiman, A.K.A., Lourenço, K.S., Clark, C., Luz, R.L., da Silva, G.H.R., Vet, L.E., Cantarella, H., Fernandes, T.V., Kuramae, E.E. 2020. From toilet to agriculture: Fertilization with microalgal biomass from wastewater impacts the soil and rhizosphere active microbiomes, greenhouse gas emissions and plant growth. Resour. Conserv. Recycl. 161: 104924. doi.org/10.1016/j.resconrec.2020.104924

Sun, T., Zhang, J.Q., Li, X., Li, M., Yang, Y., Zhou, J., Wei, Q., Zhou, B. 2021. Transcriptome and metabolome analyses revealed the response mechanism of apple to different phosphorus stresses. Plant Physiol. Biochem. 167: 639–650. doi.org/10.1016/j.plaphy.2021.08.040

Suyono, E.A., Budiman, A., Dewayanti, N., Kurnianto, D., Amelia, R. 2023. Fertilizer formulation to increase fat content in *Euglena* sp. culture and the products it produces. Ministry of Law and Human Rights of the Republic of Indonesia. Jakarta, Indonesia.

Takaichi, S. 2025. Distribution, biosynthesis, and function of carotenoids in oxygenic phototrophic algae. Mar. Drugs. 23: 62. doi.org/10.3390/md23020062

Tian, Y., Yang, K., Zheng, L., et al. 2020. Modeling biogas production kinetics of various heavy metals exposed anaerobic fermentation process using sigmoidal growth functions. Waste Biomass Valor. 11: 4837–4848. doi.org/10.1007/s12649-019-00810-x

Vadlamani, A., Viamajala, S., Pendyala, B., Varanasi, S. 2017. Cultivation of microalgae at extreme alkaline pH conditions: a novel approach for biofuel production. ACS Sustain. Chem. Eng. 5: 7284–7294. doi.org/10.1021/acssuschemeng.7b01534

Wang, N., Pei, H., Xiang, W., Li, T., Lin, S., Wu, J., Chen, Z., Wu, H., Li, C., Wu, H. 2023. Rapid screening of microalgae as potential sources of natural antioxidants. Foods. 12: 2652. doi.org/10.3390/foods12142652

Wei, C. 2024. Growth and phosphate uptake of microalgae under different phosphate conditions. E3S Web Conf. 573: 01004. doi.org/10.1051/e3sconf/202457301004

Zhang, N., Peng, D., Rui, X., Zheng, W., Zeng, Z., Huang, X., Li, C., Li, F. 2024. The effect of phosphorus concentration on the co-production of fucoxanthin and fatty acids in *Conticribra weissflogii*. Mar. Drugs. 22: 541–555. doi.org/10.3390/md22120541

Zhou, L., Jiao, C., Jilin, X., Li, Y., Chengxu, Z., Xiaojun, Y. 2017. Change of volatile components in six microalgae with different growth phases. J. Sci. Food Agric. 97: 761–769. doi.org/10.1002/jsfa.7794

Zhu, J., Hong, D.D., Wakisaka, M. 2019. Phytic acid extracted from rice bran as a growth promoter for *Euglena gracilis*. Open Chem. 17: 57–63. doi.org/10.1515/chem-2019-0006

Zhu, J., Wakisaka, M. 2020. Effect of two lignocellulose related sugar alcohols on the growth and metabolites biosynthesis of *Euglena gracilis*. Bioresour. Technol. 303: 122950. doi.org/10.1016/j.biortech.2020.122950

Zhu, J., Wakisaka, M. 2019. Finding of phytase: Understanding growth promotion mechanism of phytic acid to freshwater microalga *Euglena gracilis*. Bioresour. Technol. 296: 122343. doi.org/10.1016/j.biortech.2019.122343